J Antimicrob Chemother 2014; **69**: 1298–1310
doi:10.1093/jac/dkt534 Advance Access publication 23 January 2014

Journal of Antimicrobial Chemotherapy

Antiviral activity of baicalin against influenza virus H1N1-pdm09 is due to modulation of NS1-mediated cellular innate immune responses

Mukti Kant Nayak[1], Anurodh S. Agrawal[1], Sudeshna Bose[2], Shaon Naskar[3], Rahul Bhowmick[1], Saikat Chakrabarti[2], Sagartirtha Sarkar[3] and Mamta Chawla-Sarkar[1]*

[1]Division of Virology, National Institute of Cholera and Enteric Diseases, P-33, C.I.T. Road Scheme-XM, Beliaghata, Kolkata, West Bengal 700010, India; [2]Structural Biology and Bioinformatics Division, Council for Scientific and Industrial Research (CSIR)-Indian Institute of Chemical Biology (IICB), Kolkata, West Bengal 700032, India; [3]Department of Zoology, University of Calcutta, 35, Ballygunge Circular Road, Kolkata, West Bengal 700019, India

*Corresponding author. Tel: +91-33-2353-7470; Fax: +91-33-2370-5066; E-mail: chawlam70@gmail.com or sarkarmc@icmr.org.in

Received 11 September 2013; returned 1 November 2013; revised 11 December 2013; accepted 17 December 2013

Objectives: Baicalin, a flavonoid, has been shown to have antiviral and anti-inflammatory activities, although the mechanism of action has been unknown. Therefore, attempts were made to analyse the mechanism behind the antiviral effects of baicalin using an influenza A virus (IAV) model *in vitro* and *in vivo*.

Methods: Baicalin's anti-influenza activity was elucidated (*in vitro* and *in vivo*) utilizing pandemic influenza strain A/H1N1/Eastern India/66/pdm09 (H1N1-pdm09). Anti-influenza activity was measured by plaque inhibition, fluorescent focus-forming units (ffu) and quantifying viral transcripts using quantitative real-time PCR following treatment with baicalin in a dose- and time-dependent manner. The role of the IAV non-structural protein 1 (NS1) gene in modulating host responses was measured by immunoblotting, co-immunoprecipitation and molecular docking.

Results: Baicalin treatment following IAV infection revealed up-regulation of interferon (IFN)-induced antiviral signalling and decreased phosphoinositide 3-kinase/Akt (PI3K/Akt) activation compared with infected, untreated controls. Baicalin exerts its antiviral effects by modulating the function of the IAV-encoded NS1 protein. NS1 has been shown to counteract cellular antiviral responses by down-regulating IFN induction and up-regulating PI3K/Akt signalling. Baicalin disrupted NS1–p85β binding. Molecular docking predicted the binding site of baicalin in the RNA binding domain (RBD) of NS1. Site-directed mutagenesis within the RBD region of NS1 and the difference in the fluorescence quenching pattern of full-length NS1 and mutant NS1 proteins in the presence of baicalin confirmed the interaction of baicalin with the NS1 RBD. Amino acid residues 39–43 of the NS1 RBD were found to be crucial for the baicalin–NS1 interaction.

Conclusions: Overall, this study highlights that baicalin exerts its anti-influenza virus activity by modulating viral protein NS1, resulting in up-regulation of IFN-induced antiviral signalling and a decrease in PI3K/Akt signalling in cells.

Keywords: anti-influenza virus, flavonoids, non-structural protein 1, interferons, PI3K/Akt

Introduction

Flavonoids derived from vegetables, fruits, seeds, stems, flowers, tea, wine and honey play a protective role in human life, having antimicrobial, anti-inflammatory, antioxidant, anticancer, anticoagulant, antipyretic, antihypersensitivity and vascular protective effects.[1,2] The flavonoid baicalin, isolated from the dried root of *Scutellaria baicalensis Georgi*, has been shown to have antiviral and anticancer properties.[3–6] The anti-influenza virus activity of baicalin has been reported earlier,[7] but its mechanism of action has remained largely unknown.

Influenza A virus (IAV), belonging to the Orthomyxoviridae family, has vast genetic diversity, consisting of 17 haemagglutinin subtypes and 10 neuraminidase subtypes.[8,9] IAVs are highly contagious and pathogenic, causing annual acute respiratory disease in humans and different animal species, resulting in mortality, morbidity and huge economic loss. For the prevention of influenza, seasonal influenza vaccines are developed biannually by the WHO based on circulating strains; however, due to continuous change in influenza virus strains, the immunity provided is short-lived and vaccination of susceptible groups is required every 6

months. This results in increased vaccine costs, as well as short supply, making it largely unavailable in the developing world, where morbidity and mortality is high.[10] In addition to the vaccines, antivirals targeting the viral matrix protein M2, namely amantadine and rimantadine, and the viral neuraminidase inhibitors zanamivir and oseltamivir are available. Unfortunately, their prolonged indiscriminate use has resulted in the emergence of resistant strains.[11,12] There is thus a continued need to develop new antiviral drugs against IAV to reduce the disease burden in settings where mass vaccination is not possible.

During viral infection the innate immune response of the host cell is activated, resulting in the induction of type I interferons (IFNs), α and β, which are regulated by IFN regulatory factor 7 (IRF-7), IRF-3, NF-κB and retinoic acid inducible gene 1 (RIG-1).[13–17] The IFNs up-regulate several proteins with antiviral and pro-apoptotic roles such as signal transducer and activator of transcription 1 (STAT-1), STAT-3, STAT-5, dsRNA-dependent protein kinase R (PKR) and 2′5′-oligoadenylate synthetase 1 (OAS-1).[18–21] The influenza virus counteracts the host IFN-α/β defence mechanism with its multifunctional non-structural protein 1 (NS1).[22] Viral NS1 has two domains: the N-terminal structural RNA binding domain (RBD), consisting of three α-helices, and the C-terminal structural effector domain, consisting of seven β-strands and three α-helices. NS1 has been shown to interact with RIG-1 and PKR.[23–25] It also interacts with the p-85β subunit of phosphoinositide 3-kinase (PI3K), resulting in Akt phosphorylation and inhibition of cellular apoptosis to facilitate virus replication.[26–30]

In this study we have analysed the antiviral activity of baicalin against a pandemic IAV strain isolated in Kolkata, India—H1N1-pdm09.[31] We studied the mechanism of antiviral activity of baicalin against H1N1-pdm09 both *in vitro* (human lung carcinoma epithelial cell line, A549 cells) and *in vivo* (BALB/c mice). Our results suggest that baicalin exerts its antiviral activity by modulating the function of viral protein NS1.

Materials and methods

Cells, virus and reagents

Human lung carcinoma (A549) cells and Madin–Darby canine kidney (MDCK) cells were maintained in Dulbecco's modified Eagle's medium (DMEM) and minimal essential medium, respectively, containing 10% fetal bovine serum and antibiotics (penicillin and streptomycin) at 37°C with 5% CO_2. For virus infection, cells were washed with PBS and infected with MDCK cell culture adapted pandemic strain A/H1N1/Eastern India/66/2009 (H1N1-pdm09) in PBS containing 0.2% BSA, 1 mM $MgCl_2$, 0.9 mM $CaCl_2$, 100 U/mL penicillin and 0.1 mg/mL streptomycin for 60 min at 37°C. The inoculum was aspirated and A549 cells were incubated in infection medium supplemented with DMEM, 0.2% BSA, 0.1% trypsin and antibiotics. Baicalin (7-D-glucuronic acid-5,6-dihydroxyflavone) was purchased from Sigma–Aldrich, St Louis, MO, USA, and dissolved in DMSO for *in vitro* experiments and 0.5% sodium carboxymethyl cellulose for *in vivo* tests. The phospho-Akt (Ser 473; p-Akt; 9271S), Akt (9272S), p-IRF-3 (4947S), IRF-3 (4302S), p-STAT-3 (9167S) and SOCS-3 (2923S) antibodies were from Cell Signaling Inc., Danvers, MA, USA, the influenza A virus nucleocapsid protein (NP; sc-80481), IAV matrix 1 (M1; sc-17588), NS1 (sc-130568) and p-85β (sc-131325) antibodies were purchased from Santa Cruz Biotechnology Inc., Santa Cruz, CA, USA and the PI3K (610045) antibody from BD Biosciences, San Diego, CA, USA.

Cell viability and plaque inhibition assay in the presence of baicalin

To determine cytotoxicity of baicalin in A549 cells, cell viability assays were performed in 96-well plates with 80%–90% confluent cells (≈5×10^4 cells/well). Cells were treated with baicalin (0.5–320 μM) for 4 days followed by an MTT assay (Sigma–Aldrich). Briefly, 10 μL of MTT solution (5 mg/mL in PBS) was added and incubated at 37°C for 4 h. The formazan was dissolved in 200 μL DMSO and the optical density (OD) of the solution was measured at 570 nm and 630 nm to obtain the sample signal ($OD_{570}-OD_{630}$). The cytotoxicity was measured as loss in cell viability (TD_{50}) compared with untreated cells.

A plaque inhibition assay was carried out by seeding A549 cells into 6-well plates (≈1.2×10^6 cells per well). An equal volume of virus suspension was used, from 10-fold serial dilution of multiplicity of infection (moi) of 0.5 and 1 from virus stock (6×10^{10} pfu/L). The plates were incubated at 36°C for 60 min with frequent shaking. A 0.6% agarose overlay (3 mL) containing DMEM, trypsin (2 μg/mL) and baicalin in a range of concentrations from 1.0 μM to 120 μM was added. For the negative control, 0.1% DMSO was added in place of baicalin. Plates were incubated at 36°C in a humidified atmosphere of 5% CO_2 in air. After 72 h, plaques were stained overnight with 0.1% neutral red and plaques were counted.[32] The percentage of plaque inhibition relative to the infected, untreated control was determined for each drug concentration, and the 50% plaque inhibition concentration (IC_{50}) was determined. This experiment was performed in triplicate.

Quantifying viral transcripts and cellular genes by quantitative RT–PCR

The change in viral RNA transcripts within 24 h of virus infection was analysed. A549 cells (~2.5×10^6) were infected with H1N1-pdm09 virus as described previously (1.0 moi).[33] The inoculum was aspirated and infection medium containing 10 μM baicalin or DMSO was added. Uninfected cells treated with baicalin were used as controls. At predetermined times [4, 8, 12, 18 and 24 h post-infection (hpi)], cells were washed with PBS followed by total RNA extraction using Trizol reagent (Invitrogen, Carlsbad, CA, USA). Quantitative PCR was carried out for viral RNA quantification using a TaqMan Influenza Assay Kit (Applied Biosystems, Foster City, CA, USA) and an AgPath-ID One-Step RT–PCR Kit (Ambion, Austin, TX, USA). In order to prepare a standard curve, total RNA from 64×10^{10} pfu/L of H1N1-pdm09 was extracted. Total RNA was serially diluted (1:10) and each dilution was used as a template for real-time RT–PCR. The standard curves for viral RNA concentration were generated by plotting cycle threshold (Ct) values against 10-fold serially diluted RNA as described previously.[34] A similar method was employed for influenza virus A/Puerto Rico/8/34 (PR8) strain (80×10^{10} pfu/L of viral stock). The same set of RNA was used to estimate IFN-α, IFN-β, RIG-1, interleukin-8 (IL-8), tumour necrosis factor α (TNF-α), PKR, IRF-3, OAS-1, ribonuclease L (RNase L) and 18S rRNA using TaqMan Gene Expression assays (Applied Biosystems) according to the manufacturer's protocol. The change in amplification of the target gene was normalized to the 18S rRNA. The fold expression in the target host gene was calculated by using $2^{-\Delta\Delta Ct}$ formula.[35]

Western blot analysis

The A549 cells were infected with H1N1-pdm09 virus as mentioned earlier (1.0 moi and 5.0 moi)[33] and treated with baicalin at 10 μM or DMSO. At the indicated time post-infection, A549 cell monolayers were washed with PBS and whole-cell lysates were prepared, and immunoblotting was done as per standard protocols described previously.[36] The membrane was probed with the primary antibodies against NP, p-Akt, p-IRF-3, p-PKR, RIG-1, p-STAT-3 and NS1. Blots were reprobed with IRF-3, glyceraldehyde 3-phosphate dehydrogenase (GAPDH) or Akt antibody to confirm equal protein loading. All immunoblots were done at least three times to confirm

results. The band intensity was measured by using Quantity One version 4.6.3 software (Bio-Rad, Hercules, CA, USA).

Antiviral activity of baicalin in an in vivo mouse model

Male BALB/c mice (18–22 g) aged 6 weeks were obtained from the National Centre for Laboratory Animal Sciences, National Institute of Nutrition, Jamai-Osmania, Hyderabad, India and maintained in the animal care facility of the University of Calcutta, Kolkata. The experiments with animals were conducted in accordance with the Institutional Animal Ethics Committee guidelines, University of Calcutta (Registration #885/ac/05/CPCSEA), Kolkata, registered under 'Committee for the Purpose of Control and Supervision of Experiments on Laboratory Animals', Ministry of Environment and Forests, Government of India and conformed with the *Guide for the Care and Use of Laboratory Animals* published by the US NIH (Publication No. 85-23, revised 1996). The mice were anaesthetized by inhalation of diethyl ether and intranasally infected with 50 μL of 4×50% murine lethal dose (MLD_{50}) of H1N1-pdm09 strain in PBS. Twenty-four hours after virus inoculation, the mice ($n=3$ per dose) were treated with increasing concentrations of baicalin (10–120 mg/kg/day) by oral gavage twice daily for 3 days, as described previously.[7] On the fourth day the mice were sacrificed, and lung homogenates were analysed for infective virus titre using a haemagglutination assay using 1% (v/v) guinea-pig red blood cells with a detection limit of 10 $TCID_{50}$/mL.[37] The decrease in virus titre relative to the infected untreated control mice was determined for each drug concentration, and the 50% inhibitory concentration for mice (MIC_{50}) was determined. The viral titres were further confirmed using the fluorescent focus-forming unit (ffu) assay in MDCK cells following infection with 10-fold serial dilutions of the supernatant of lung homogenates according to the method described by Moriyama and Sorokin.[38] NP antibody and Goat anti-Mouse IgG (H+L) Secondary Antibody DyLight 488 conjugate (35502; Thermo Fisher Scientific Inc., Pierce Antibody, Rockford, IL USA) were used for staining and ffu were counted under a fluorescent microscope (Carl Zeiss, Axio Imager). A fresh group of BALB/c mice ($n=12$) were infected with H1N1-pdm09 strain followed by treatment with either baicalin (40 mg/kg/day; $n=6$) or DMSO (vehicle control; $n=6$) as described earlier. As control, uninfected mice ($n=6$) were treated with baicalin (40 mg/kg/day). After 24 h of baicalin treatment, the mice were sacrificed and lungs were homogenized in modified radioimmunoprecipitation buffer (phenylmethylsulfonyl fluoride, protease inhibitor and phosphatase inhibitor cocktail) for western blotting to determine the relative amounts of p-Akt and M1 protein in respective treatment groups (virus infected; DMSO treated, virus infected; baicalin treated and uninfected; baicalin treated). This experiment was performed in triplicate.

Plasmid, transfection and baicalin treatment

The NS1 gene (accession no. GU983274)[31] of H1N1-pdm09 was cloned in pcDNA 6/V5 (Invitrogen). The pcD-NS1 (1 μg) or pcDNA6 vector was transfected in A549 cells in a 35 mm dish with Lipofectamine 2000 (Invitrogen) according to the manufacturer's protocol. Four hours after transfection, cells were either treated with baicalin (0.5–16 μM) or left untreated for 24 h. Whole-cell lysates were prepared and immunoblotting was performed to detect p-Akt and NS1 protein quantity, as described previously.[36]

Co-immunoprecipitation

A549 cells either transfected with pcD-NS1 or infected with H1N1-pdm09 (at 1.0 moi) and treated with 10 μM baicalin or DMSO for 24 h were lysed in a solution containing 10 mM Tris (pH 8.0), 170 mM NaCl, 0.5% NP-40 and protease inhibitors for 30 min on ice. Cell debris was removed by centrifugation, and the supernatants were clarified by incubation (2 h at 4°C) with protein A-Sepharose beads (Sigma–Aldrich) followed by centrifugation. Beads were discarded and supernatants were incubated with anti-NS1 antibody overnight at 4°C followed by protein A-Sepharose for a further 4 h. Beads were washed four times with 1 mL of wash buffer (200 mM Tris pH 8.0, 100 mM NaCl and 0.5% Nonidet P-40), and bound proteins were eluted with SDS sample buffer and separated on 12% SDS-polyacrylamide gels. Blots were immunoblotted with anti-p-85β antibody as described previously.[39] All experiments were performed three times.

Protein–ligand docking and sequence alignment

The amino acid sequence of A/H1N1/Eastern India/66/pdm09 (ADD85869) strain (RBD amino acids 1–81 and effector domain amino acids 82–205) was used in the study. The full-length NS1 protein structure was generated by combination of the three-dimensional (3D) coordinates of the N-terminus (PDB ID: 3M8A) and C-terminus (PDB ID: 3M5R) of the H1N1 NS1 protein using MODELLER software.[40] The model was filtered based on the lowest energy parameters (MOLPDF and DOPE scores) and were further validated using PROCHECK[41] and Verify 3D[42] structural validation tools. The validated model structure of the full-length NS1 protein was further refined by molecular dynamics simulation using GROMOS96 53a6 force field of the GROMACS v4.5.3 package.[43] The simulation protocol involved energy minimization of the system using steepest descent followed by conjugate gradient algorithms. The production run was performed with an NPT ensemble [at physiological temperature (300 K) and pressure (1 bar)]. The system, comprising the whole protein and the solvent, was separately coupled to the temperature bath to ensure minimal fluctuations in the simulation temperature. The total production run of 100 ns took 170 CPU hours using four nodes (each having six Intel Zeon X5675 processors) of a high performance computing (HPC) machine cluster. The refined and equilibrated structure of the NS1 protein was used for docking analysis. Molecular docking of baicalin with NS1 proteins was performed using PatchDock[44,45] and GOLD v5.1[46] docking software using default parameters. The sequence alignment was carried by using BioEdit version 7.0.9.0. software.[47]

In vitro transcription, translation and purification

The vectors pcD-NS1, pcD-NS1-RBD (nucleotides 1–234) and pcD-NS1-effector domain (nucleotides 235–657) were subjected to *in vitro* coupled transcription and translation using the TNT Quick Coupled Transcription/Translation system (Promega, Madison, WI, USA) according to the manufacturer's protocol. Recombinant proteins were purified using a Ni-NTA Spin Kit (Qiagen, Hilden, Germany) under native conditions according to the kit protocol.

Fluorescence spectroscopy

Purified full-length NS1, NS1-RBD and NS1-effector domain were incubated with baicalin to form complexes between protein and ligand as described previously.[48] The fluorescence emission spectra of the complex at different concentrations of baicalin and NS1 protein were recorded in the wavelength range 300–450 nm, with the excitation wavelength at 290 nm, using a fluorescence spectroscope (Photon Technology International). Buffer was used as a corresponding blank to correct the background fluorescence.

Site-directed mutagenesis

Four individual nucleotide substitution mutations (C103G, A120C, T124C and A136G) in the pcD-NS1 vector were created using the QuickChange II Site-Directed Mutagenesis kit (Agilent Technologies, Inc., Santa Clara, CA, USA) following the manufacturer's protocol. Mutant proteins were purified on an Ni-NTA Spin Kit (Qiagen) following the kit protocol. To analyse the baicalin binding properties of these mutants, mutant

protein–baicalin complexes were generated and fluorescence spectroscopy carried out as described earlier. The full-length NS1 protein–baicalin complex was taken as a positive control.

Statistical analysis

The data are expressed as mean ± SD of at least three independent experiments. Statistical analysis was performed using Student's *t*-test. In all tests, $P<0.05$ was considered statistically significant.

Results

Baicalin shows potent anti-influenza activity both in vitro and in vivo in mice

To assess the biological function of any potential drug candidate, its effect on cellular homeostasis needs to be evaluated. Thus, the effect of baicalin on cell viability was assessed by the MTT assay. Briefly, A549 cells were treated with increasing concentrations of baicalin (0.5–320 μM) and incubated for 96 h. Cell viability was measured with respect to vehicle-treated (DMSO) controls by the MTT assay. As shown in Figure S1 (available as Supplementary data at *JAC* Online), 50% cell viability (TD_{50}) was observed at 220 μM ± 10 μM of baicalin. The IC_{50} (50% virus reduction) of H1N1-pdm09 strain (0.5 moi) *in vitro* in A549 cells by the pfu method was observed at ≈18 μM baicalin after 72 h (Figure 1a). *In vivo*, BALB/c mice were infected intranasally with the H1N1-pdm09 strain, followed by treatment with increasing concentrations of baicalin (10–120 mg/kg/day) twice daily for 3 days. Lung homogenates were analysed for viral titre by both the haemagglutination assay and ffu in MDCK cells. MIC_{50} by the ffu assay was calculated to be ≈80 mg/kg/day (Figure 1b). To rule out any non-specific toxic effects, 10 μM and 40 mg/kg/day

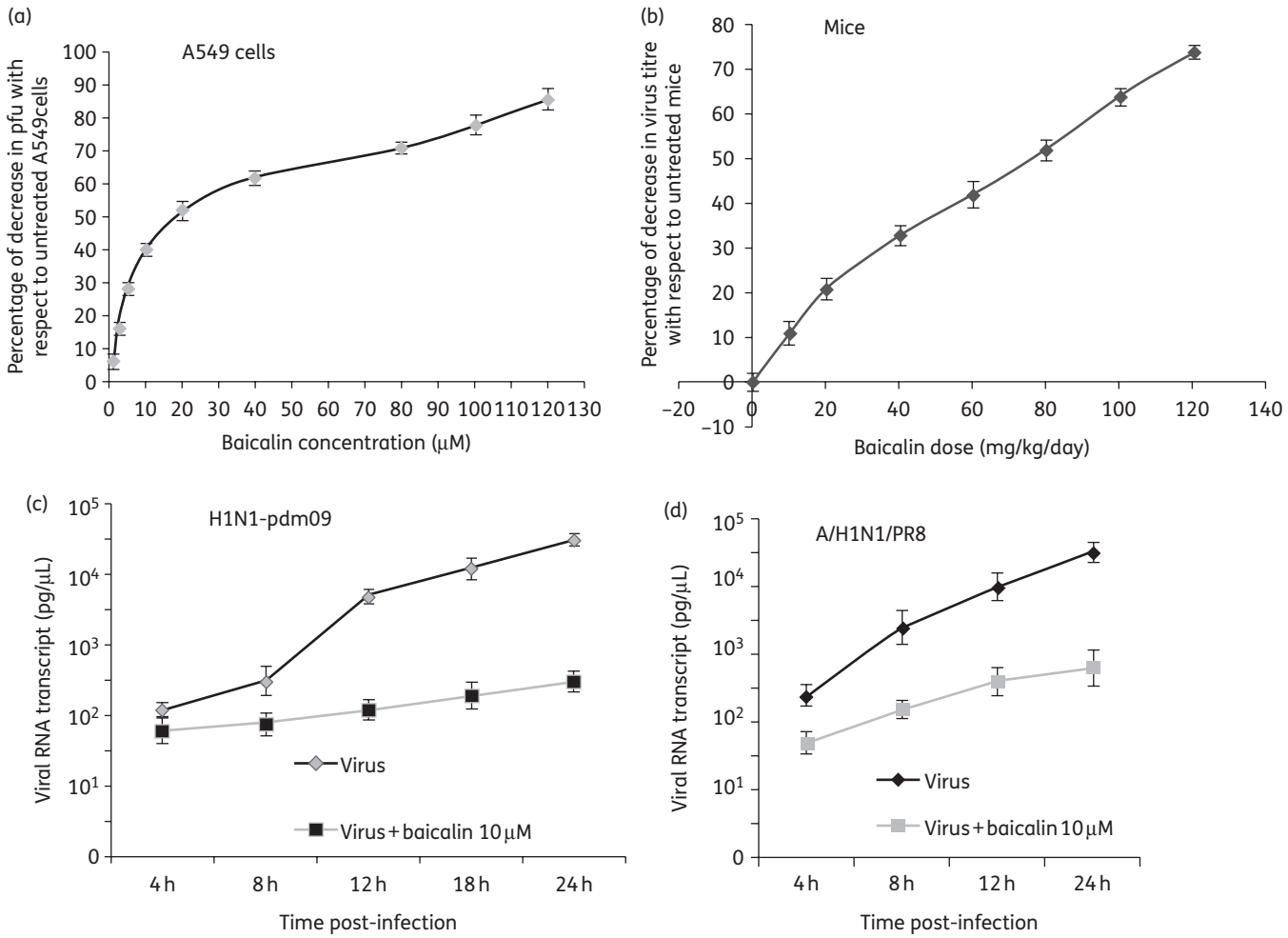

Figure 1. Baicalin inhibits virus growth. (a) Baicalin IC_{50} was assessed by plaque assay in A549 cells infected with the H1N1-pdm09 virus at 10-fold serial dilution of 0.5 moi in the presence and absence of baicalin (1.0–120 μM). After 72 h, the numbers of plaques were counted and are presented as the percentage decrease with respect to untreated cells. (b) Antiviral activity of baicalin in mice. Viral titre in lungs of mice infected with H1N1-pdm09 (50 μL of $4\times MLD_{50}$) for 72 h in the presence of baicalin (10–120 mg/kg/day) or DMSO vehicle as determined using the ffu assay. (c and d) Expression of viral transcripts of the NP gene was quantified by real-time RT–PCR in A549 cells infected with H1N1-pdm09 (1.0 moi) (c) or H1N1/PR8 (1.0 moi) (d) in the presence or absence of baicalin (10 μM). Fold change was estimated by standard curve of H1N1-pdm09 RNA. Briefly, a 10-fold serial dilution of total RNA from 64×10^{10} pfu/L was transcribed by real-time RT–PCR for the NP gene. Ct values are based on 10-fold serial dilutions of H1N1-pdm09 total RNA template. Results are representative of three independent experiments. $P<0.05$ was considered statistically significant.

of baicalin were used *in vitro* and *in vivo*, respectively, since a significant decrease (40%) in virus titre was observed (Figure 1a and b). Inhibition of virus growth was assessed indirectly by measuring transcript levels of NP (viral RNA) by quantitative PCR in the presence or absence of baicalin. At 24 hpi with H1N1-pdm09 (at 1.0 moi) an ≈100-fold reduction in viral NP transcript was observed in the presence of baicalin (10 μM) (Figure 1c), while a ≈60-fold reduction was observed in A549 cells infected with the IAV PR8 strain (Figure 1d). Antiviral effects of baicalin were also observed in cells infected with higher moi (5 moi) (data not shown).

Effect of baicalin on IFN-induced signalling in IAV-infected cells

Cells recognize virus infection and trigger innate immunity as the first line of defence. Induction of the innate immune response was assessed by analysing the expression levels of cytokines such as type I IFNs (α and β) and representative genes, namely RIG-1, IRF-3 and PKR in the presence or absence of baicalin in a post-infection time-course study. In uninfected A549 cells, no change in the expression level of IFNs was observed following treatment with baicalin. A549 cells infected with H1N1-pdm09 (1.0 moi) in

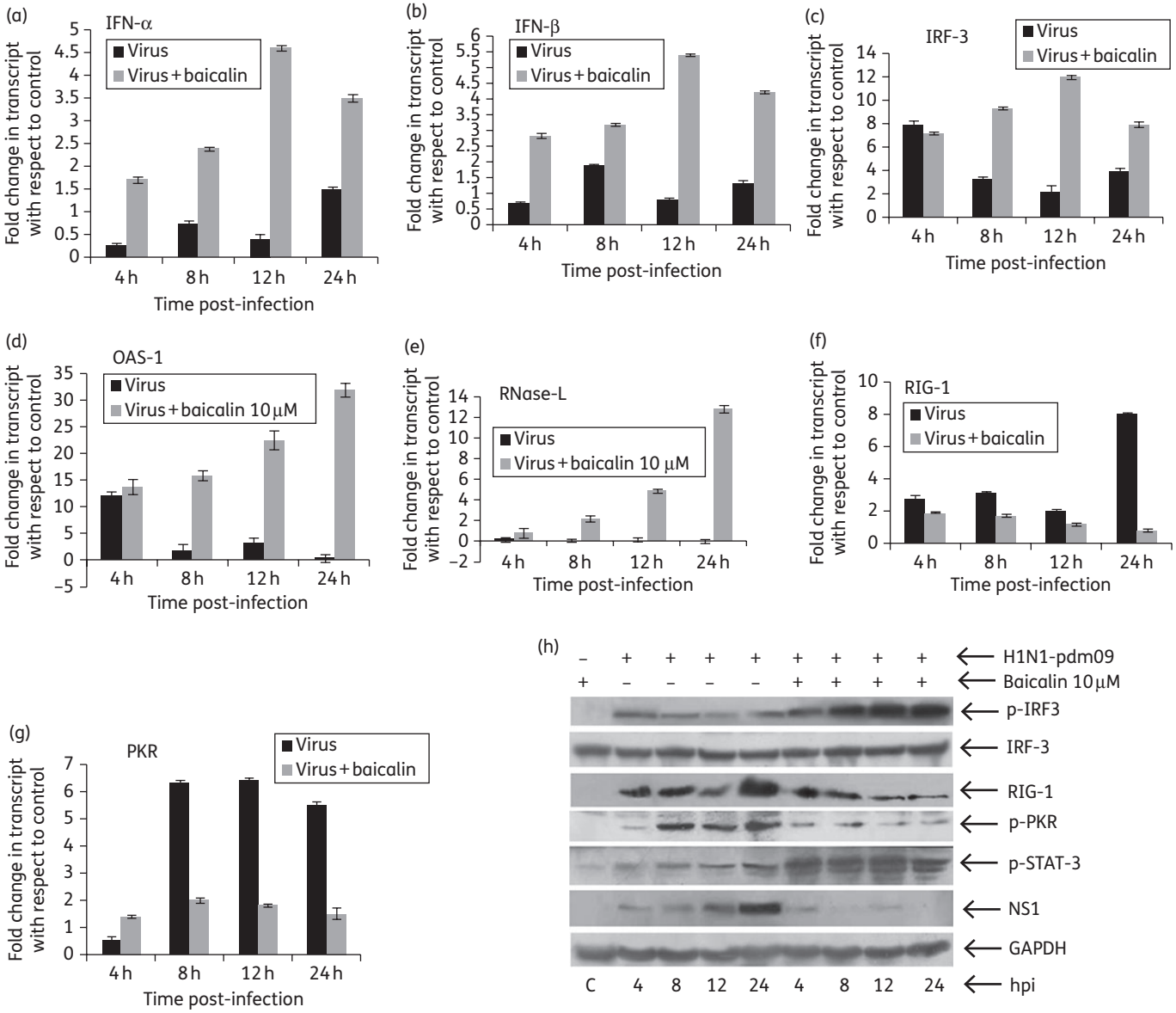

Figure 2. Effect of baicalin on IAV-induced IFN signalling in cells. The change in expression of (a) IFN-α, (b) IFN-β, (c) IRF-3, (d) OAS-1, (e) RNase L, (f) RIG-1 and (g) PKR transcripts in A549 cells infected with 1.0 moi of the H1N1-pdm09 strain in the presence or absence of 10 μM baicalin was measured by real-time PCR using TaqMan probes. The expression of transcripts was calculated in relation to the expression level of 18S rRNA and expressed as a fold change compared with mock-treated cells. (h) Immunoblot analysis was done in cell lysates of A549 cells infected with the H1N1-pdm09 strain (1.0 moi) followed by treatment with or without baicalin (10 μM) to assess the expression of NS1, p-IRF3, IRF-3, RIG-1, p-PKR, p-STAT-3 and GAPDH. The blot shown is representative of three independent experiments. $P < 0.05$ was considered statistically significant.

the presence or absence of baicalin (10 μM), revealed a time-dependent increase in expression of IFN-α and IFN-β in the presence of baicalin compared with uninfected cells (Figure 2a and b). By contrast, the expression of antiviral genes RIG-1 and PKR was significantly lower in cells treated with baicalin (Figure 2f and g), whereas that of IRF-3, a regulator of IFN, OAS-1 and RNase L, was significantly higher in the presence of baicalin (Figure 2c–e). Furthermore, to assess IFN-induced signalling, cell lysates of A549 cells infected with H1N1-pdm09 (1.0 moi) in the presence or absence of baicalin were subjected to western blotting to analyse the expression of NS1, p-IRF3, RIG-1, p-PKR and p-STAT3. Consistent with previous results, expression of the viral protein NS1 was significantly lower in the presence of baicalin, confirming reduced viral replication. By contrast, transcription factor IRF-3 and STAT3 were phosphorylated in cells treated with baicalin compared with untreated cells (Figure 2h and Figure S2, available as Supplementary data at *JAC* Online). Total IRF-3 and GAPDH expression remained unchanged in the presence or absence of baicalin. Consistent with the transcript levels, RIG-1 and p-PKR protein were down-regulated in virus-infected cells treated with baicalin compared with untreated cells (Figure 2h and Figure S2, available as Supplementary data at *JAC* Online). The pro-inflammatory cytokines TNF-α and IL-8 were also significantly lower in the presence of baicalin compared with untreated virus-infected cells (Figure 3a and b). Overall results suggest that baicalin modulates IFN activation in cells, resulting in inhibition of virus replication and a subsequent decrease in pro-inflammatory or antiviral genes.

Role of baicalin in down-regulating a negative regulator of cytokine signalling and virus-induced PI3K/Akt pathways

Viruses also modulate cellular apoptosis, by activating the survival pathway during the early stages of infection.[49] The effect of baicalin on the IAV-induced SOCS-3 and PI3K/Akt pathway in A549 cells was therefore assessed following H1N1-pdm09 infection. Cell lysates prepared in a time-dependent manner were subjected to western blotting using an antibody specific for SOCS-3 and p-Akt (Ser 473). Unlike IFN, relative fold decreases in SOCS-3 (5.61-fold) and p-Akt (5.36-fold) expression were detected in baicalin-treated cells compared with untreated cells at 24 hpi (Figures 3c and 4a). The decrease in p-Akt correlated with reduced IAV protein (NP) expression in cells, suggesting overall inhibition of viral replication (Figure 4a). No change in expression of total Akt was observed during IAV infection in the presence or absence of baicalin. To further confirm the effect of baicalin on PI3K activity, cell lysates prepared from mouse lung infected with H1N1-pdm09 (50 μL of 4×MLD_{50}) (24 hpi) followed by treatment with baicalin (40 mg/kg/day) or DMSO were subjected to western blotting to assess the expression of viral protein M1 and p-Akt. Consistent with *in vitro* results, the expression of M1 and p-Akt was significantly decreased in baicalin-treated mice compared with untreated mice (Figure 4b). Overall results suggest that reduced virus replication in the presence of baicalin results in inhibition of virus-induced pro-survival pathways.

Baicalin modulates the function of IAV NS1 protein

IAV NS1 protein has been shown to regulate virus-induced Akt/PI3K and IFN signalling.[26–29] Here, we observed that baicalin modulates both virus-induced Akt phosphorylation and IFN expression, and therefore the effect of baicalin on NS1 protein was analysed. The NS1 gene of H1N1-pdm09 was cloned in pcDNA6 (pcD-NS1) and transfected in A549 cells. Only vector (pcDNA6) or pcD-NS1 transfected cells were either treated with baicalin or left untreated. After 24 h, cell lysates were prepared and immunoblot analysis was done to assess p-Akt. In the absence of baicalin, increased Akt phosphorylation was observed in NS1-expressing cells, whereas in the presence of baicalin it was significantly lower, suggesting disruption of NS1 protein function (Figure 4c).

Whole-cell lysates of A/H1N1/2009-infected cells (treated or untreated with baicalin) were immunoprecipitated with anti-NS1 antibody followed by immunoblotting with the antibody-specific p-85β subunit of PI3K. As shown in Figure 4d, a significantly lower amount of p-85β immunoprecipitated with NS1 in the presence of baicalin compared with untreated cells. This was further confirmed in pcD-NS1-expressing A549 cells, where p-85β co-immunoprecipitated with NS1 in the absence of

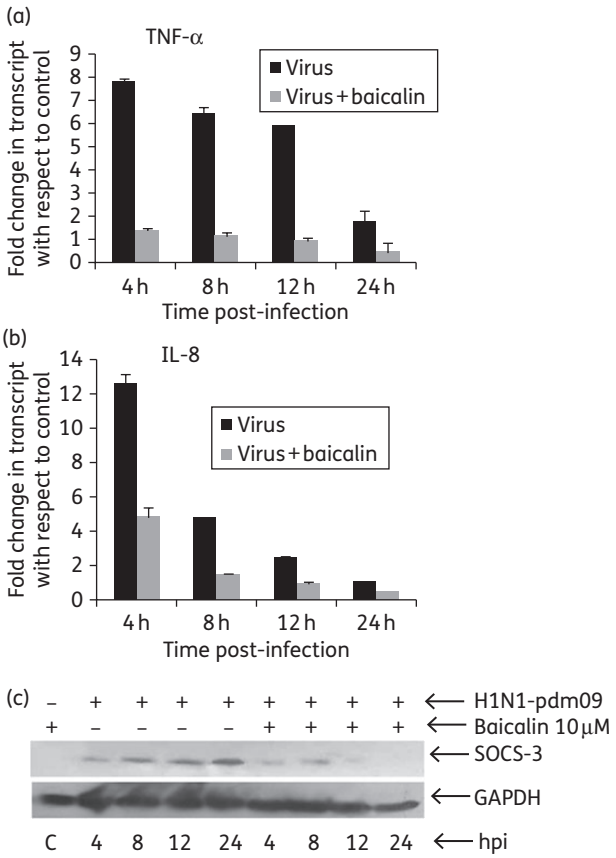

Figure 3. Effect of baicalin on pro-inflammatory cytokines and cytokine suppressors. A549 cells were infected with the H1N1-pdm09 strain at 1.0 moi and incubated with or without baicalin (10 μM). The transcripts encoding human (a) TNF-α and (b) IL-8 were measured by real-time PCR using TaqMan probes and expressed as the fold change after normalizing with respect to 18S rRNA. (c) The cell lysates prepared at specific times post-infection were subjected to western blotting using SOCS-3 and GAPDH antibodies. Results are representative of three independent experiments. $P<0.05$ was considered statistically significant.

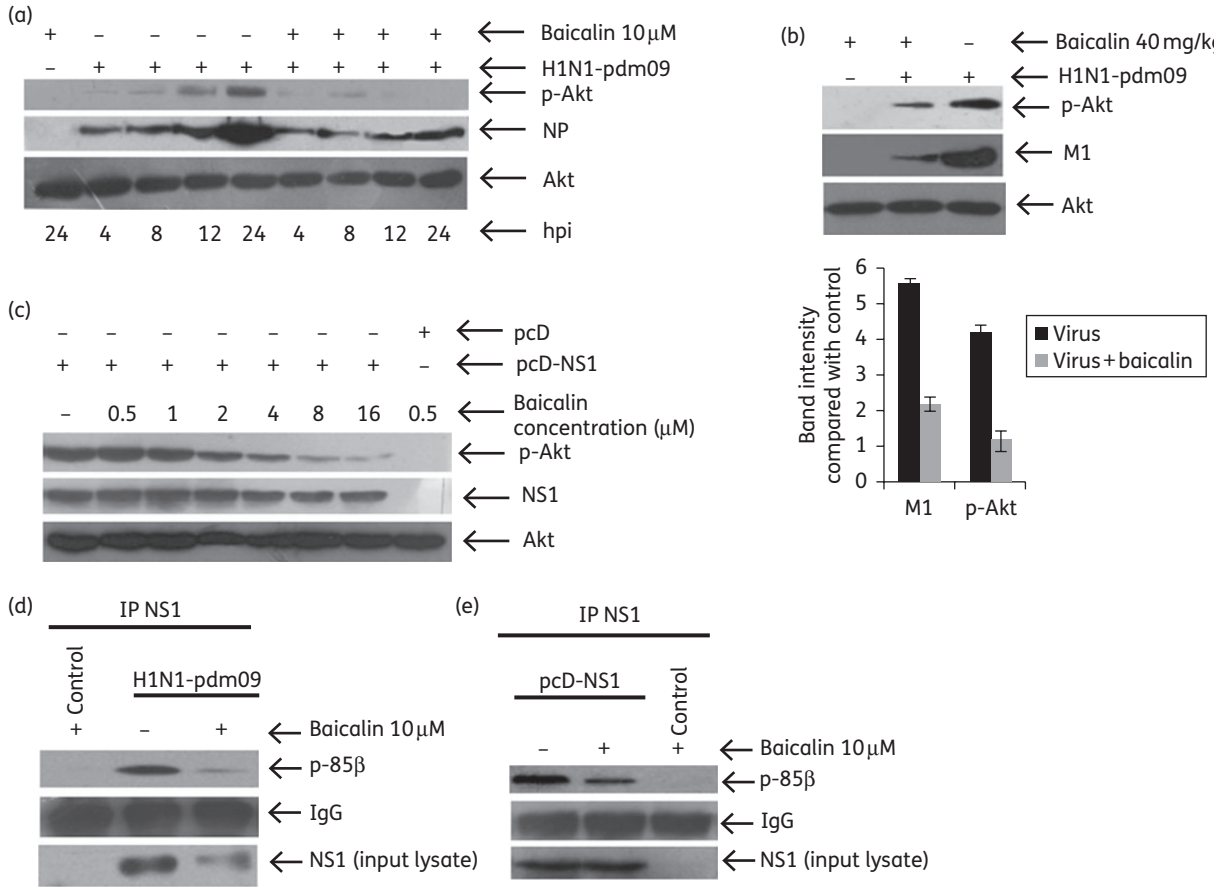

Figure 4. Effect of baicalin *in vitro* and *in vivo* on NS1-induced Akt phosphorylation. (a) A549 cells infected with the H1N1-pdm09 strain at 1.0 moi were incubated with or without baicalin (10 μM). Cell lysates prepared at specific times post-infection were subjected to western blotting using phospho-Akt (Ser 473), NP and Akt antibodies. (b) Effect of baicalin on the PI3K/Akt pathway during influenza virus infection was evaluated in BALB/c mice by treating the mice with baicalin at 40 mg/kg/day and, after 24 h, subjecting lung homogenates to western blotting using phospho-Akt (Ser 473), M1 and Akt antibodies. Band intensity was quantified using Quantity One software. (c) A549 cells transfected with pcD-NS1 or vector (pcDNA6) control were incubated with or without baicalin (0.5–16 μM). Cell lysates prepared after 24 h were subjected to western blotting using phospho-Akt (Ser 473), NS1 and Akt antibodies. (d) The serum-starved A549 cells infected with H1N1-pdm09 (1.0 moi) were treated with baicalin (10 μM) or DMSO vehicle for 24 h. The NS1 was immunoprecipitated using NS1 antibody and immunoblotted with p-85β antibody to confirm association. (e) A549 cells transfected with pcD-NS1 or empty vector (pcDNA6) control were treated with baicalin (10 μM) or DMSO (control) for 24 h. Cell lysates were subjected to immunoprecipitation with NS1 antibody and immunoblotted with p-85β antibody. The membrane was reprobed with anti-mouse secondary antibody as a loading control for immunoprecipitation. The blot shown is representative of three independent experiments. $P < 0.05$ was considered statistically significant.

baicalin, but reduced interaction was observed in the presence of baicalin (Figure 4e). Overall results thus suggest that baicalin inhibits p-85β–NS1 binding, resulting in reduced Akt phosphorylation.

Prediction of the binding site of baicalin with NS1 protein

Since baicalin inhibited the NS1–p-85β interaction, it was hypothesized that baicalin may bind to the same region of NS1 to out-compete p-85β. A computational simulation study was therefore carried out to predict the interacting region within NS1. Since the crystal structure of the whole NS1 protein is not available, the structure of the full-length NS1 protein was generated by combination of the 3D coordinates of the N-terminus (PDB ID: 3M8A) and C-terminus (PDB ID: 3M5R) of the H1N1 NS1 protein using MODELLER[40] software (Figure 5a) followed by molecular dynamics simulation-based refinement using the GROMACS v4.5.3 package.[43] The ligand baicalin was docked to the full-length NS1 protein, NS1 effector domain and the RBD independently. A blind or naive docking approach employed by PatchDock[44,45] software suggested that baicalin has a relatively higher binding probability for the RBD than the effector domain (Figure 5b). Further, a residue-specific docking approach employed by the GOLD v5.1 program[46] suggested that region 35–46 of helix 2 within the NS1-RBD covers the binding region. Involvement of amino acids R35, R38, D39, Q40, S42 and R46 in the interaction with baicalin was predicted (Figure 5c). The docking study also suggested the probability of hydrogen bond formation between baicalin and three arginine

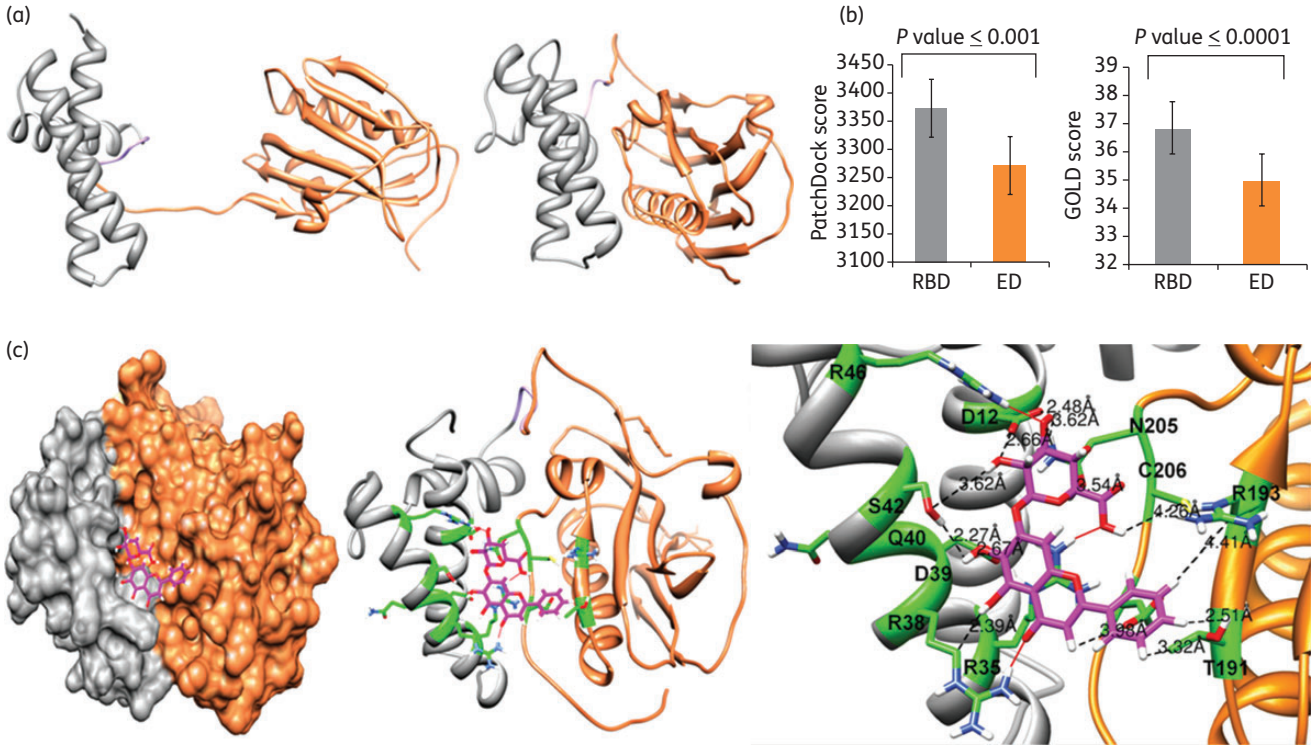

Figure 5. Full-length NS1 structure and docking analysis. (a) The predicted 3D structure of the NS1 protein consists of the RBD (grey) and the effector domain (orange). The model structure became significantly compact (right side) after it was subjected to 100 ns of molecular dynamic simulation using GROMOS96 53a6 force field of the GROMACS v4.5.3 package.[43] (b) The molecular docking program suggested higher binding probability for baicalin with respect to the RBD than the effector domain of NS1 when baicalin was docked to the full-length NS1 protein (left) and to the effector domain (ED) and the RBD independently (right). (c) Probable binding position of baicalin in the RBD of the NS1 protein as suggested by GOLD v5.1 docking software.[46] Residues within 5 Å distance (D12, R35, R38, D39, S42, R46, T191, R193, N205, C206 and E208) from the docked baicalin are shown in green and the residues within 5–10 Å (S8, F9, V11, L15, W16, R19, D34, Q40, K41, L43, V192, V194, W203, R204 and D207) are shown, while probable hydrogen bonds are indicated by red lines. This figure appears in colour in the online version of *JAC* and in black and white in the print version of *JAC*.

residues of the NS1 full-length protein at positions 35, 38 and 46, respectively.

Baicalin interacts with amino acid region 39–43 of the RBD of NS1

Spectroscopy was used to confirm the possible binding between NS1 and baicalin, as predicted by the molecular docking experiment. Purified full-length NS1 protein, NS1-RBD and NS1-effector domain revealed strong fluorescence emission peaks at 331, 339 and 330 nm, respectively, after excitation at 290 nm. When a fixed concentration of NS1 protein was incubated with increasing amounts of baicalin, a remarkable decrease in the intrinsic fluorescence of the NS1–baicalin and NS1-RBD–baicalin complexes was observed (Figure 6a and b). Furthermore, a slight shift in the maximum wavelength of whole NS1 protein and NS1-RBD fluorescence emission was observed in the presence of baicalin. The interaction between the effector domain of NS1 and baicalin did not show any significant change compared with the NS1-effector domain alone (Figure 6c). Once it was confirmed that baicalin interacted with NS1-RBD, four mutants of NS1 (namely R35G, Q40H, S42P and R46G) were constructed by site-directed mutagenesis. Spectral emission profiles of the mutants compared with NS1 were analysed in the presence or absence of baicalin. NS1 mutants Q40H and S42P did not show any significant changes in fluorescence intensity in the presence or absence of baicalin, unlike full-length NS1 or NS1-RBD, where quenching of fluorescence was observed in the presence of baicalin. This suggests that amino acids Q40 and S42 are crucial for NS1–baicalin binding (Figure 7a and b). The R35G and R46G mutants showed quenching of fluorescence intensity in the presence of baicalin similar to full-length NS1 protein (data not shown). To further confirm this within the cell, A549 cells were transfected with constructs encoding NS1 mutants (namely pcD-Q40H-NS1, pcD-S42P-NS1 and pcD-R46G-NS1) in the presence of 10 μM baicalin. After 24 h, cell lysates were co-immunoprecipitated with NS1 antibody followed by immunoblotting with p-85β subunit antibody. As an internal control, p-85β–NS1 interaction in cells transfected with full-length pcD-NS1 was analysed. In the presence of baicalin, NS1 mutants pcD-Q40H-NS1 and pcD-S42P-NS1 showed strong interaction with p-85β, whereas NS1 mutant pcD-R46G-NS1 revealed a significantly lower interaction with p-85β, which is consistent with the spectroscopy data (Figure 7c), suggesting that mutation in the 39–43 amino acid region of NS1 reduces the NS1–baicalin interaction. Overall, the results confirmed the interaction of baicalin with NS1 in the 39–43 amino acid region, which disrupts the NS1–p85β interaction.

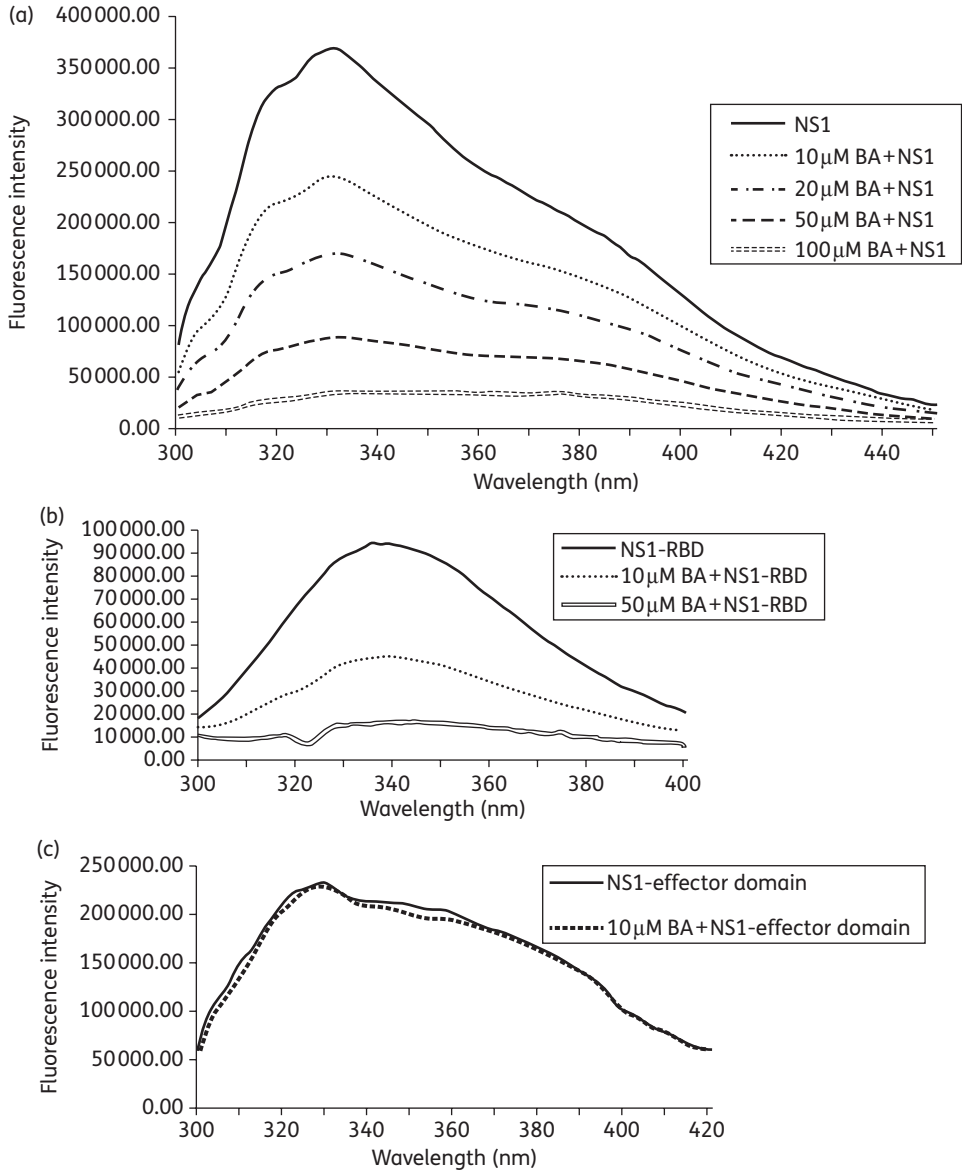

Figure 6. Analysis of NS1–baicalin binding by fluorescence spectroscopy. Full-length NS1 (a), NS1-RBD (b) and NS1-effector domain (c) were incubated with baicalin (BA) (10–100 μM) at pH 8.0. The change in spectral shift was analysed by excitation at a wavelength of 290 nm and emission at a wavelength of 300–450 nm. Results are representative of three independent experiments.

Discussion

The plant extract baicalin has been shown to have anti-influenza viral activity both *in vivo* and *in vitro*.[7,50] Its antiviral effects on hepatitis B virus, HIV-1 and herpes simplex virus-1 (HSV-1) *in vitro* have also been reported,[3,51–53] although the mechanism of action has been relatively unknown. Consistent with previous results, the present study also showed antiviral effects of baicalin against human IAV (H1N1-pdm09) both *in vitro* and *in vivo* (Figure 1a–c).

Host cells induce type I IFN as a first line of defence against virus infection, but most viruses have evolved strategies to block the IFN response as a means to increase their replication efficiency.[54] The IAV inhibits IFN production through the NS1 protein.[55] The NS1 protein has two domains: the RBD and the effector domain. A number of amino acids, including Arg 38, Lys 41, Thr 5, Pro 31, Asp 34, Arg 35, Gly 45, Arg 46 and Thr 49 in the RBD region have been predicted to interact with RNA.[56,57] The NS1-RBD binds to RIG-1/interferon-β promoter stimulator 1 (IPS-1)[23,58,59] and blocks downstream signalling,[60,61] resulting in attenuation of type I IFN and inflammatory cytokine expression. It also binds to dsRNA and prevents activation of IRF-3, IFN synthesis[62] and the OAS-1-dependent RNase L pathway.[63] The IAV has been shown to inhibit cellular pro-inflammatory responses such as TNF-α, IL-8 and IFNs.[64–69] Consistent with previous reports, induction of IFN-α, IFN-β and IRF-3 was attenuated in A549 cells at 8–12 hpi with IAV-pdm09 (Figure 2a–c and h, and Figure S2, available as Supplementary data at *JAC* Online);

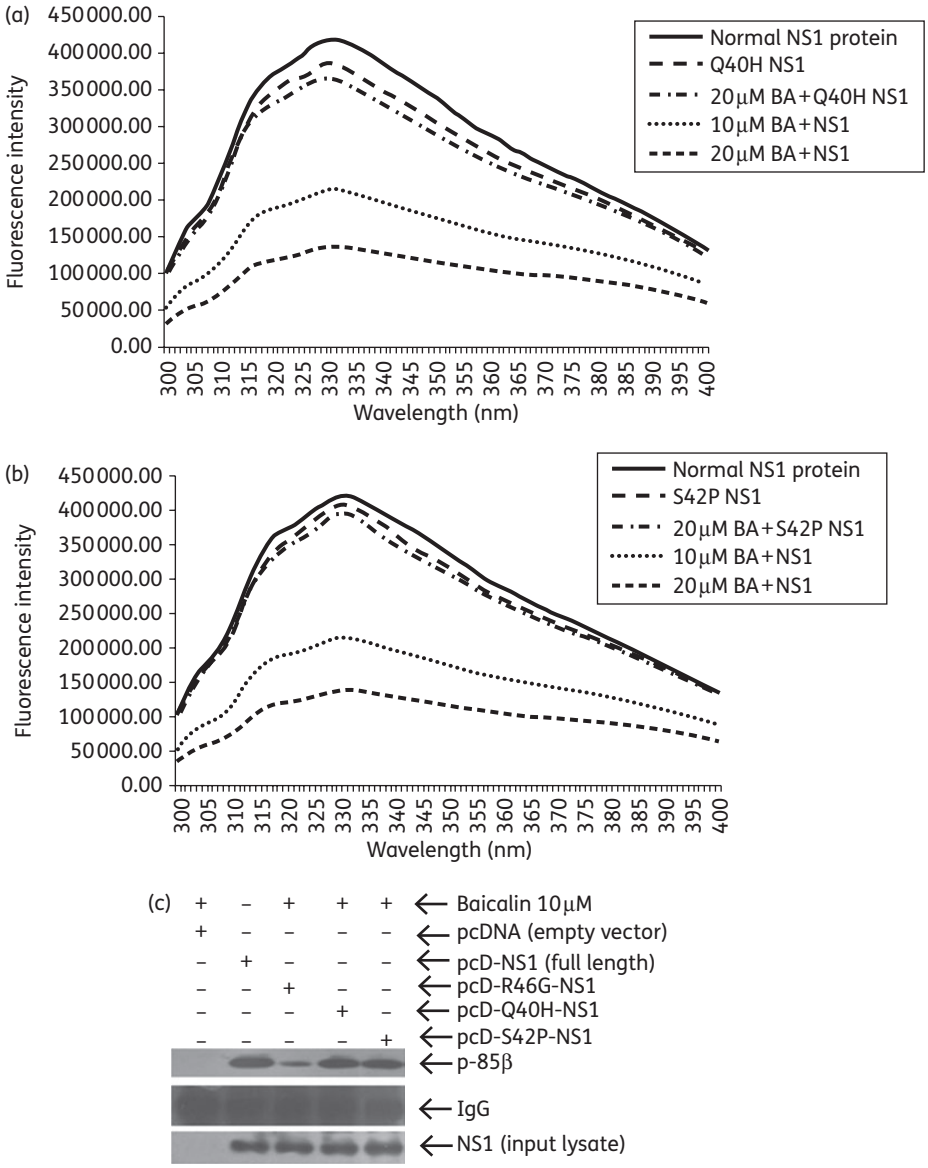

Figure 7. Glutamine (at position 40) and serine (at position 42) interact with NS1. Analysis of the change in fluorescence spectroscopy spectra, by excitation at a wavelength of 290 nm and emission at a wavelength of 300–400 nm, of NS1 protein (a and b), Q40H NS1 mutant (a) and S42P NS1 mutant (b) in the presence or absence of baicalin (BA), revealed that changes in amino acids at positions 40 and 42 disrupted the binding of NS1 and baicalin. (c) A549 cells transfected with pcD-R46GNS1, pcD-Q40H-NS1, pcD-S42P-NS1 or empty vector (pcDNA6) and treated with baicalin (10 μM) for 24 h. For a positive control, A549 cells transfected with full-length pcD-NS1 in the absence of baicalin were used. Cell lysates were subjected to immunoprecipitation with NS1 antibody and immunoblotted with p-85β antibody. Cell lysates were immunoblotted with NS1 to confirm expression of NS1 in transfected cells. Results are representative of three independent experiments.

however, in the presence of baicalin, the expression of IFN-α, IFN-β and IRF-3 was high even at 24 hpi. IFN activates RNase L, which degrades viral RNA and results in inhibition of viral replication.[70–72] The activation of RIG-1/IPS-1 is dependent on cytosolic viral RNA, IFN-inducible laboratory of genetics and physiology 2 (LGP2) and IFN-induced 15 kDa protein (ISG15), which controls RIG-1 function and synthesis to maintain a balance between innate defence and hypersensitivity during antiviral responses.[17,73–75] Thus in baicalin-treated cells, IFN and RNase L levels were high, whereas RIG-1 was inhibited (Figure 2f and h, and Figure S2, available as Supplementary data at *JAC* Online). Owing to the induction of IFN in the presence of baicalin, IAV replication was attenuated, resulting in decreased viral transcripts (Figure 1c and d) and low levels of pro-inflammatory cytokines TNF-α and IL-8 (Figure 3a and b). Similarly, PKR expression was low, which could be due to both increased p-STAT3 activity, which suppresses autophagy through PKR, as well as reduced viral replication.[76] In addition to the IRF-3/RNase L pathway, NS1 also modulates IFN induction through activation of the SOCS-3 protein,[77,78] which is consistent with our results in which reduced SOCS-3 expression

was observed in the presence of baicalin. Other than IFN regulation, NS1 interacts with p-85β through its Src homology 3 (SH3) binding motif 1 to activate the PI3K/Akt pathway.[79] Baicalin was shown to inhibit NS1–p-85β interaction, as well as Akt phosphorylation, suggesting that baicalin may exert its anti-influenza activity by disrupting NS1 functions (Figure 4a–e).

Since NS1–PI3K binding was inhibited in the presence of baicalin, molecular docking was carried out to identify the binding domain of NS1, which may interact with baicalin. The results suggested direct interaction between the NS1-RBD and baicalin through hydrogen bonding at second helical structure (Figure 5c). Site-directed mutagenesis of residues in the predicted domain (35, 40, 42 and 46 amino acid) followed by fluorescence spectroscopy and co-immunoprecipitation confirmed the importance of the 39–43 amino acid region within NS1-RBD for this interaction (Figure 7a–c). Binding with NS1 in the RBD region might possibly disrupt the RNA binding function of NS1, which may result in dsRNA-mediated induction of IRF-3, IFNs and RNase L in cells to create an antiviral state. In addition, binding of baicalin to the RBD may modulate the structure of NS1 so that the SH3 region within the effector domain of NS1 is not freely available for interaction with p-85β. The importance of the RBD was further confirmed by alignment of NS1 protein sequences of H1N1-pdm09, H1N1, H5N1, H6N1, H9N2 and PR8 influenza virus strains, which revealed the highly conserved nature of a region comprising amino acids 37–47 in all subtypes except H5N1, where only one amino acid substitution (at 41) was observed (Figure S3, available as Supplementary data at *JAC* Online).

The antiviral effects of baicalin have been reported previously in many RNA viruses,[3,7,52] suggesting it has broad antiviral activity. The present study highlights the mechanism of the anti-influenza virus effect of baicalin during IAV infection. Baicalin induces its antiviral effects by modulating the function of multifunction protein NS1, which regulates host innate immune responses.[21–28,57–62] Since NS1 is a relatively conserved protein in IAV, antiviral drugs targeting NS1 will probably have a lower risk of generating drug-resistant mutants, unlike exisiting drugs targeting surface antigens. Although further studies are required to analyse the structure–function relationship between baicalin and the NS1 protein, baicalin can be developed as a potential anti-influenza drug based on the results from a previous study[7] as well as the current study.

Acknowledgements

We sincerely thank Dr Kalyan K. Banerjee and Amarshi Mukherjee (Division of Biochemistry, NICED) for their valuable inputs with regard to the baicalin–NS1 interaction studies.

Funding

This study was supported by the Indian Council of Medical Research (ICMR), India and the University of Calcutta, India.

Transparency declarations

None to declare.

Supplementary data

Figures S1, S2 and S3 are available as Supplementary data at *JAC* Online (http://jac.oxfordjournals.org/).

References

1 Cushnie TPT, Lamb AJ. Antimicrobial activity of flavonoids. *Int J Antimicrob Agents* 2005; **26**: 343–6.

2 Havsteen BH. The biochemistry and medical significance of the flavonoids. *Pharmacol Ther* 2002; **96**: 67–202.

3 Cheng Y, Ping J, Xu HD *et al*. Synergistic effect of a novel oxymatrine-baicalin combination against hepatitis B virus replication, α smooth muscle actin expression and type I collagen synthesis in vitro. *World J Gastroenterol* 2006; **12**: 5153–9.

4 Chan FL, Choi HL, Chen ZY *et al*. Induction of apoptosis in prostate cancer cell lines by a flavonoid, baicalin. *Cancer Lett* 2000; **160**: 219–28.

5 Dong LH, Wen JK, Miao SB *et al*. Baicalin inhibits PDGF-BB-stimulated vascular smooth muscle cell proliferation through suppressing PDGFRβ-ERK signaling and increase in p27 accumulation and prevents injury-induced neointimal hyperplasia. *Cell Res* 2010; **20**: 1252–62.

6 Xu XF, Cai BL, Guan SM *et al*. Baicalin induces human mucoepidermoid carcinoma Mc3 cells apoptosis in vitro and in vivo. *Invest New Drugs* 2011; **29**: 637–45.

7 Xu G, Dou J, Zhang L *et al*. Inhibitory effects of baicalein on the influenza virus in vivo is determined by baicalin in the serum. *Biol Pharm Bull* 2010; **33**: 238–43.

8 Tong S, Li Y, Rivailler P *et al*. A distinct lineage of influenza A virus from bats. *Proc Natl Acad Sci USA* 2012; **109**: 4269–74.

9 Wright PF, Neumann G, Kawaoka Y. Orthomyxoviruses. In: Fields BN, Knipe D, Howley P, eds. *Fields Virology*. 5th edn. Lippincott Williams & Wilkins, 2007; 1692–740.

10 Couch RB. Seasonal inactivated influenza virus vaccines. *Vaccine* 2008; **26**: 5–9.

11 Poland GA, Jacobson RM, Ovsyannikova IG. Influenza virus resistance to antiviral agents: a plea for rational use. *Clin Infect Dis* 2009; **48**: 1254–6.

12 Agrawal AS, Sarkar M, Ghosh S *et al*. Genetic characterization of circulating seasonal influenza A viruses (2005–2009) revealed introduction of oseltamivir resistant H1N1 strains during 2009 in eastern India. *Infect Genet Evol* 2010; **10**: 1188–98.

13 Marié I, Durbin JE, Levy DE. Differential viral induction of distinct interferon-α genes by positive feedback through interferon regulatory factor-7. *EMBO J* 1998; **17**: 6660–9.

14 Sato MH, Suemori N, Hata M *et al*. Distinct and essential roles of transcription factors IRF-3 and IRF-7 in response to viruses for IFN-α/β gene induction. *Immunity* 2000; **13**: 539–48.

15 Fitzgerald KA, McWhirter SM, Faia KL *et al*. IKKε and TBK1 are essential components of the IRF3 signaling pathway. *Nat Immunol* 2003; **4**: 491–6.

16 Sharma S, tenOever BR, Grandvaux N *et al*. Triggering the interferon antiviral response through an IKK-related pathway. *Science* 2003; **300**: 1148–51.

17 Chiu YH, Macmillan JB, Chen ZJ. RNA polymerase III detects cytosolic DNA and induces type I interferons through the RIG-I pathway. *Cell* 2009; **138**: 576–91.

18 van Boxel-Dezaire AH, Zula JA, Xu Y *et al*. Major differences in the responses of primary human leukocyte subsets to IFN-β. *J Immunol* 2010; **185**: 5888–99.

19 Garcia MA, Gil J, Ventoso I *et al*. Impact of protein kinase PKR in cell biology: from antiviral to antiproliferative action. *Microbiol Mol Biol Rev* 2006; **70**: 1032–60.

20 Clemens MJ. Translational control in virus-infected cells: models for cellular stress responses. *Semin Cell Dev Biol* 2005; **16**: 13–20.

21 Silverman RH. Viral encounters with OAS and RNase L during the IFN antiviral response. *J Virol* 2007; **81**: 12720–9.

22 Garcia-Sastre A, Egorov A, Matassov D *et al*. Influenza A virus lacking the NS1 gene replicates in interferon-deficient systems. *Virology* 1998; **252**: 324–30.

23 Mibayashi M, Martinez-Sobrido L, Loo YM *et al*. Inhibition of retinoic acid-inducible gene-I-mediated induction of β interferon by the NS1 protein of influenza A virus. *J Virol* 2007; **81**: 514–24.

24 Gack MU, Albrecht RA, Urano T *et al*. Influenza A virus NS1 targets the ubiquitin ligase TRIM25 to evade recognition by the host viral RNA sensor RIG-I. *Cell Host Microbe* 2009; **5**: 439–49.

25 Li S, Min JY, Krug RM *et al*. Binding of the influenza A virus NS1 protein to PKR mediates the inhibition of its activation by either PACT or double-stranded RNA. *Virology* 2006; **349**: 13–21.

26 Hale BG, Jackson D, Chen Y *et al*. Influenza A virus NS1 protein binds p85β and activates phosphatidylinositol-3-kinase signaling. *Proc Natl Acad Sci USA* 2006; **103**: 14194–9.

27 Shin YK, Liu Q, Tikoo SK *et al*. Influenza A virus NS1 protein activates the phosphatidylinositol 3-kinase (PI3K)/Akt pathway by direct interaction with the p-85 subunit of PI3K. *J Gen Virol* 2007; **88**: 13–8.

28 Shin YK, Liu Q, Tikoo SK *et al*. Effect of the phosphatidylinositol 3-kinase/Akt pathway on influenza A virus propagation. *J Gen Virol* 2007; **88**: 942–50.

29 Hale BG, Batty IH, Downes CP *et al*. Binding of influenza A virus NS1 protein to the inter-SH2 domain of p85 suggests a novel mechanism for phosphoinositide 3-kinase activation. *J Biol Chem* 2008; **283**: 1372–80.

30 Yao R, Cooper GM. Requirement for phosphatidylinosotol-3 kinase in the prevention of apoptosis by nerve growth factor. *Science* 1995; **267**: 2003–6.

31 Sarkar M, Agrawal AS, Sharma Dey R *et al*. Molecular characterization and comparative analysis of pandemic H1N1/2009 strains with co-circulating seasonal H1N1/2009 strains from eastern India. *Arch Virol* 2011; **156**: 207–17.

32 Hayden FG, Cote KM, Douglas RG Jr. Plaque inhibition assay for drug susceptibility testing of influenza viruses. *Antimicrob Agents Chemother* 1980; **17**: 865–70.

33 Wang J, Nikrad MP, Phang T *et al*. Innate immune response to influenza A virus in differentiated human alveolar type II cells. *Am J Respir Cell Mol Biol* 2011; **45**: 582–91.

34 Yang JH, Lai JP, Douglas SD *et al*. Real-time RT–PCR for quantitation of hepatitis C virus RNA. *J Virol Methods* 2002; **102**: 119–28.

35 Huang C, Yang L, Li Z *et al*. Detection of CCND1 amplification using laser capture microdissection coupled with real-time polymerase chain reaction in human esophageal squamous cell carcinoma. *Cancer Genet Cytogenet* 2007; **175**: 19–25.

36 Dutta D, Bagchi P, Chatterjee A *et al*. The molecular chaperone heat shock protein-90 positively regulates rotavirus infection. *Virology* 2009; **391**: 325–33.

37 Rowe T, Banner D, Farooqui A *et al*. In vivo ribavirin activity against severe pandemic H1N1 influenza A/Mexico/4108/2009. *J Gen Virol* 2010; **91**: 2898–906.

38 Moriyama T, Sorokin A. BK virus (BKV): infection, propagation, quantitation, purification, labeling, and analysis of cell entry. *Curr Protoc Cell Biol* 2009; Chapter 26: Unit 26.2.

39 Bagchi P, Nandi S, Nayak MK *et al*. Molecular mechanism behind rotavirus NSP1-mediated PI3 kinase activation: interaction between NSP1 and the p85 subunit of PI3 kinase. *J Virol* 2013; **87**: 2358–62.

40 Šali A, Potterton L, Yuan F *et al*. Evaluation of comparative protein modeling by MODELLER. *Proteins* 1995; **23**: 318–26.

41 Laskowski RA, MacArthur MW, Moss DS *et al*. PROCHECK: a program to check the stereochemical quality of protein structures. *J Appl Crystallogr* 1993; **26**: 283–91.

42 Eisenberg D, Luthy R, Bowie JU. VERIFY3D: assessment of protein models with three-dimensional profiles. *Methods Enzymol* 1997; **277**: 396–404.

43 Van Der Spoel D, Lindahl E, Hess B *et al*. GROMACS: fast, flexible, and free. *J Comput Chem* 2005; **26**: 1701–18.

44 Duhovny D, Nussinov R, Wolfson HJ. Efficient unbound docking of rigid molecules. In: Gusfield *et al*., eds. *Proceedings of the Second Workshop on Algorithms in Bioinformatics (WABI)*, Rome, Italy. Springer Verlag, Lecture Notes in Computer Science 2002; 2452: 185–200.

45 Schneidman-Duhovny D, Inbar Y, Nussinov R *et al*. PatchDock and SymmDock: servers for rigid and symmetric docking. *Nucleic Acids Res* 2005; **33**: 363–7.

46 Jones G, Willett P, Glen RC *et al*. Development and validation of a genetic algorithm for flexible docking. *J Mol Biol* 1997; **267**: 727–48.

47 Hall TA. BioEdit: a user-friendly biological sequence alignment editor and analysis program for Windows 95/98/NT. *Nucleic Acids Symp Ser* 1999; **41**: 95–8.

48 Mishra B, Barik A, Priyadarsini KI *et al*. Fluorescence spectroscopic studies on binding of a flavonoid antioxidant quercetin to serum albumins. *J Chem Sci* 2005; **117**: 641–7.

49 Ehrhardt C, Wolff T, Pleschka S *et al*. Influenza A virus NS1 protein activates the PI3K/Akt pathway to mediate antiapoptotic signaling responses. *J Virol* 2007; **81**: 3058–67.

50 Chu ZY, Chu M, Teng Y. Effect of baicalin on in vivo anti-virus. *Zhongguo Zhong Yao Za Zhi* 2007; **32**: 2413–5.

51 Li BQ, Fu T, Gong WH *et al*. The flavonoid baicalin exhibits anti-inflammatory activity by binding to chemokines. *Immunopharmacology* 2000; **49**: 295–306.

52 Lyu SY, Rhim JY, Park WB. Antiherpetic activities of flavonoids against herpes simplex virus type 1 (HSV-1) and type 2 (HSV-2) in vitro. *Arch Pharm Res* 2005; **28**: 1293–301.

53 Zhao J, Zhang ZP, Chen HS *et al*. Preparation and anti-HIV activity study of baicalien and its benzylated derivatives. *Yao Xue Xue Bao* 1997; **32**: 140–3.

54 Bonjardim CA, Ferreira PC, Kroon EG. Interferons: signaling, antiviral and viral evasion. *Immunol Lett* 2009; **122**: 1411.

55 Hale BG, Randall RE, Ortin J *et al*. The multifunctional NS1 protein of influenza A viruses. *J Gen Virol* 2008; **89**: 2359–76.

56 Wang W, Riedel K, Lynch P *et al*. RNA binding by the novel helical domain of the influenza virus NS1 protein requires its dimer structure and a small number of specific basic amino acids. *RNA* 1999; **5**: 195–205.

57 Yin C, Khan JA, Swapna GV *et al*. Conserved surface features form the double-stranded RNA binding site of non-structural protein 1 (NS1) from influenza A and B viruses. *J Biol Chem* 2007; **282**: 20584–92.

58 Guo Z, Chen LM, Zeng H *et al*. NS1 protein of influenza A virus inhibits the function of intra cytoplasmic pathogen sensor, RIG-I. *Am J Respir Cell Mol Biol* 2007; **36**: 263–9.

59 Opitz B, Rejaibi A, Dauber B *et al*. IFN-β induction by influenza A virus is mediated by RIG-I which is regulated by the viral NS1 protein. *Cell Microbiol* 2007; **9**: 930–8.

60 Ludwig S, Wang X, Ehrhardt C *et al*. The influenza A virus NS1 protein inhibits activation of Jun N-terminal kinase and AP-1 transcription factors. *J Virol* 2002; **76**: 11166–71.

61 Wang X, Li M, Zheng H *et al*. Influenza A virus NS1 protein prevents activation of NF-κβ and induction of α/β interferon. *J Virol* 2000; **74**: 11566–73.

62 Talon J, Horvath CM, Polley R *et al*. Activation of interferon regulatory factor 3 is inhibited by the influenza A virus NS1 protein. *J Virol* 2000; **74**: 7989–96.

63 Min JY, Krug RM. The primary function of RNA binding by the influenza A virus NS1 protein in infected cells: inhibiting the 2′-5′ oligo (A) synthetase/RNase L pathway. *Proc Natl Acad Sci USA* 2006; **103**: 7100–5.

64 Sprenger H, Meyer RG, Kaufmann A *et al*. Selective induction of monocyte and not neutrophil-attracting chemokines after influenza A virus infection. *J Exp Med* 1996; **184**: 1191–6.

65 Matsukura S, Kokubu F, Noda H *et al*. Expression of IL-6, IL-8, and RANTES on human bronchial epithelial cells, NCI-H292, induced by influenza virus A. *J Allergy Clin Immunol* 1996; **98**: 1080–7.

66 Kaiser L, Fritz RS, Straus SE *et al*. Symptom pathogenesis during acute influenza: interleukin-6 and other cytokine responses. *J Med Virol* 2001; **64**: 262–8.

67 Ronni T, Sareneva T, Pirhonen J *et al*. Activation of IFN-α, IFN-γ, MxA, and IFN regulatory factor 1 genes in influenza A virus-infected human peripheral blood mononuclear cells. *J Immunol* 1995; **154**: 2764–74.

68 Bender A, Amann U, Jager R *et al*. Effect of granulocyte/macrophage colony-stimulating factor on human monocytes infected with influenza A virus enhancement of virus replication, cytokine release, and cytotoxicity. *J Immunol* 1993; **151**: 5416–24.

69 Geiss GK, Salvatore M, Tumpey TM *et al*. Cellular transcriptional profiling in influenza A virus-infected lung epithelial cells: The role of the nonstructural NS1 protein in the evasion of the host innate defense and its potential contribution to pandemic influenza. *Proc Natl Acad Sci USA* 2002; **99**: 10736–41.

70 Rutherford MN, Hannigan GE, Williams BR. Interferon-induced binding of nuclear factors to promoter elements of the 2-5A synthetase gene. *EMBO J* 1988; **7**: 751–9.

71 Zhou A, Hassel BA, Silverman RH. Expression cloning of 2-5A-dependent RNAase: a uniquely regulated mediator of interferon action. *Cell* 1993; **72**: 753–65.

72 Floyd-Smith G, Slattery E, Lengyel P. Interferon action: RNA cleavage pattern of a (2′-5′)oligoadenylate-dependent endonuclease. *Science* 1981; **212**: 1030–2.

73 Yoneyama M, Kikuchi M, Matsumoto K *et al*. Shared and unique functions of the DExD/H-box helicases RIG-I, MDA5, and LGP2 in antiviral innate immunity. *J Immunol* 2005; **175**: 2851–8.

74 Saito T, Hirai R, Loo YM *et al*. Regulation of innate antiviral defenses through a shared repressor domain in RIG-I and LGP2. *Proc Natl Acad Sci USA* 2007; **104**: 582–7.

75 Kim MJ, Hwang SY, Imaizumi T *et al*. Negative feedback regulation of RIG-I-mediated antiviral signaling by interferon-induced ISG15 conjugation. *J Virol* 2008; **82**: 1474–83.

76 Shen S, Niso-Santano M, Adjemian S *et al*. Cytoplasmic STAT3 represses autophagy by inhibiting PKR activity. *Mol Cell* 2012; **48**: 667–80.

77 Pauli EK, Schmolke M, Wolff T *et al*. Influenza A virus inhibits type I IFN signaling via NF-kappaB-dependent induction of SOCS-3 expression. *PLoS Pathog* 2008; **4**: e1000196.

78 Jia D, Rahbar R, Chan RW *et al*. Influenza virus non-structural protein 1 (NS1) disrupts interferon signaling. *PLoS One* 2010; **5**: e13927.

79 Shin YK, Li Y, Liu Q *et al*. SH3 binding motif 1 in influenza A virus NS1 protein is essential for PI3K/Akt signalling pathway activation. *J Virol* 2007; **81**: 12730–9.